

# DIRECT NUMERICAL SIMULATION OF TRANSITIONAL –TURBULENT FLOW WITH HEAT TRANSFER IN A CLOSED ROTOR-STATOR CAVITY

**Eric Serre, Patrick Bontoux**

Laboratoire de Modélisation et Simulation Numérique en Mécanique L3M  
IMT - La Jetée ; Technopôle de Château-Gombert; 38 rue Frédéric Joliot-Curie,  
F-13451 Marseille Cedex 20, France  
[serre1@L3m.univ-mrs.fr](mailto:serre1@L3m.univ-mrs.fr), [bontoux@L3m.univ-mrs.fr](mailto:bontoux@L3m.univ-mrs.fr)

**Brian Launder**

Department of Mechanical, Aerospace & Manufacturing Engineering  
Manchester M60 1QD, UK  
[brian.launder@umist.ac.uk](mailto:brian.launder@umist.ac.uk)

## ABSTRACT

In this paper, a non-isothermal flow confined between a rotating and a stationary disc is investigated using direct numerical simulation. Besides its fundamental importance as a three-dimensional prototype flow, such flows frequently arise in many industrial devices, especially in turbomachinery applications. The direct numerical simulation is performed by integrating the time-dependent Navier-Stokes equations with a three-dimensional spectral method. The effects of thermal convection have been examined for a transitional turbulent flow at  $Re(=\Omega R_1^2/\nu)=110000$  in an annular cavity of aspect ratio  $L(=\Delta R/H)=2.35$ . These DNS results provide accurate, instantaneous quantities which may be helpful in understanding the physics of turbulent flow and heat transfer in a rotating disc cavity. Moreover, the averaged results provide target data for workers employing RANS schemes.

## INTRODUCTION

The problem of heat transfer in turbulent and transitional flow in rotating systems is of great engineering importance, particularly for designing rotating machinery, e.g., turbines electrical machinery and generator rotors. Fundamental investigations that are relevant to the cooling of gas turbines and turbomachinery are reported in monographs by (Owen & Rogers, 1989a,b). A better knowledge of the characteristics of these types of flow is a key factor in the performance of many industrial devices. Typical configurations are cavities between rotating compressors or turbines discs, between counter-rotating discs, and in rotor-stator systems with or without throughflow. The flow created in the gap between rotating discs controls the distribution of temperature within the cavity which, in turn, affects the performance and reliability of the machine.

A recently recognized feature of such flows is that highly structured, large-scale precessing vortices may be set up within the disc cavity, which seem certain to have a large effect on the resultant heat-transfer coefficients at the disc surface. It is thus essential to understand these large-scale

motions, and the mechanisms that control them, and how they affect the drag and heat transfer on the discs and contribute to the performance of the device (Owen, 2000).

The steady laminar heat transfer and fluid flow in co-rotating or stationary disc systems has been extensively investigated theoretically and experimentally (see the review by Yan and Lee, 1997). Both numerical and experimental results indicated a considerable augmentation in heat transfer by rotation-induced Coriolis effects. Turbulent heat and momentum transport has been studied experimentally by Elkins and Eaton (2000) in a single disc flow. Mean velocity and Reynolds stress measurements agreed well with previous isothermal studies showing that temperature, for the conditions of their experiment with small temperature differences, may be considered negligible.

When attention shifts to an enclosed rotor-stator cavity a characteristic feature is the coexistence of adjacent coupled flow regions that are radically different in terms of the flow properties and the thickness scales of the Ekman and Bödewadt layers (adjacent to the rotating and fixed discs, respectively) compared to those of the geostrophic core region (Brady & Durlofsky, 1986; Serre *et al.*, 2001). In real situations the isothermal flow between the discs undergoes a transition to turbulence when the local Reynolds number  $Re_r = \Omega r^2/\nu$ , based on the radial coordinate  $r$ , is sufficiently large. The precise radial position of this transition depends both on  $Re_r$  and the aspect ratio,  $L$ . A characteristic of the rotor-stator flow is that the Bödewadt becomes turbulent at a lower Reynolds number than the Ekman. In an experiment where the boundary layers on the two discs do not merge ( $L=12.5$ ), Itoh *et al.* (1992) found that the rotor layer was laminar for  $Re_r = 1.6 \times 10^5$ , partly turbulent for  $Re_r = 3.6 \times 10^5$  and fully turbulent for  $Re_r = 4.6 \times 10^5$ . Thus, the structure of these flows is highly complex involving laminar, transitional and turbulent flow regions. Moreover, as a consequence of confinement, of flow curvature and rotational effects, the turbulence is strongly inhomogeneous and anisotropic.

In this paper, a non-isothermal flow confined between a rotating and a stationary disc is investigated numerically. This

kind of flow is of interest as a quite simple arrangement for investigating three-dimensional turbulent boundary-layer physics and as a benchmark that can be used in modelling more complex flows directly relevant to rotating machinery (Iacovides and Toumpanakis, 1993). The effects of thermal convection have been examined for a transitional turbulent flow at  $Re(=\Omega R_1^2/\nu)=110000$  in an annular cavity of aspect ratio  $L(=\Delta R/H)=2.35$ . These DNS results provide accurate, instantaneous quantities which may be helpful in understanding the physics of turbulent flow and heat transfer in a rotating disc cavity. Moreover, the averaged results provide target data for workers employing RANS schemes.

Our slightly longer term aim is to include the effects of density variation as this introduces a quasi-buoyant effect on the near-wall layers due to the radial acceleration,  $O^2r$ . None of the detailed experimental studies of disc-cavity flows have examined this effect due to the extreme flow conditions arising in an actual gas turbine. As a preliminary exploration we here show the modest effects of a Rayleigh number  $\sim 10^4$ . It is hoped that in the oral presentation of this work it will be possible to show the influence of a much stronger centrifugal field characteristic of modern turbomachinery.

## GEOMETRICAL AND MATHEMATICAL MODELS

The geometry considered is that of two discs enclosing an annular domain of radial extent  $\Delta R=R_1-R_0$ , where  $R_0$  and  $R_1$  are the internal and the external radii, respectively. Two cylinders of height  $H$  bound the solution domain, the inner one being rotating while the outer one is at rest; the origin of the  $z$ -axis is located at mid-height between the discs. The internal and external cylinders are termed the shaft and the shroud, respectively. The upper disc of the cavity rotates at uniform angular velocity  $\Omega=\Omega e_z$  while the other is at rest. This configuration that is an idealisation of a turbine cavity element, is an attractive configuration for numerical studies because the boundary conditions are well defined, the flow being completely enclosed. Consequently, the flow is disturbance-free and well-controlled numerical experiments can be carried out.

Two parameters define the geometry: these may be taken as the curvature parameter  $Rm=(R_1+R_0)/\Delta R$  and the aspect ratio  $L=\Delta R/H$ . In this work  $L=2.35$  and  $Rm=2.33$ . These values correspond to a practical compromise between actual rotor-stator devices (that are of larger aspect ratio) and the computational cost of the numerical simulation.

The equations governing the flow in this configuration are the 3D Navier-Stokes equations written in the velocity-pressure formulation, together with the continuity and energy equations. Appropriate boundary and initial conditions are provided with these equations.

It is convenient to write these using a cylindrical polar coordinate system  $(r, z, \theta)$ , relative to a stationary observer with the origin at the centre of the cylinder. The velocity components are,  $u, v, w$ , and  $p$  is the pressure. The scales for the dimensionless variables of space, time, velocity and temperature are  $[H/2, \Omega^{-1}, \Omega R_1, (T_{hot}+T_{cold})/2]$ , respectively. The dimensionless axial and radial coordinates are  $z=2z^*/H, -1=z=1$  and  $r=2r^*/H, L(Rm-1)=r=L(Rm+1)$ , respectively. The radius and the temperature has been normalised on  $[-1, 1]$ , a requirement for the use of Chebyshev polynomials.

No-slip boundary conditions apply at all walls; there  $u=w=0$ . For the tangential velocity, the boundary conditions are  $v=0$  on the stator ( $z=-1$ ) and  $v=(Rm+r)/(Rm+1)$  on the rotating disc ( $z=1$ ). On the shroud (outer cylinder)  $v=0$  and on the shaft (inner cylinder),  $v=\Omega R_0$ , which corresponds to the more unstable geometrical configuration. The junction of the outer cylinder at rest with the rotor (or the rotating inner cylinder with the stator) involves a singularity of the tangential velocity. This singular condition expresses a physical situation where there is a thin gap between the edge of the rotating disc and the stationary sidewall. Unless this singularity is treated appropriately, spectral methods may have severe difficulties dealing with it and an exponential function has been considered in order to regularize this condition. The gravity vector points in the negative  $z$  direction and is thus orthogonal to the upper (cold rotor) and lower discs (hot stator) which are maintained at uniform temperature. On the cylindrical surfaces the temperature is prescribed as varying linearly between  $T_{hot}$  at the lower surface to  $T_{cold}$  at the upper.

The flow dynamics depends on four parameters: the Reynolds number ( $Re$ ), the Rayleigh number ( $Ra$ ), the Froude ( $Fr$ ) number and the Prandtl number ( $Pr$ ) defined as  $Re=\Omega R_1^2/\nu$ ,  $Ra=g\alpha\Delta TH^3/\nu\kappa$ ,  $Pr=\nu/\kappa$  and  $Fr=\Omega^2 R_1/g$ , where  $\Delta T, \alpha, \nu$  and  $\kappa$  are, respectively, the temperature difference between the discs, the thermal expansion coefficient, kinematic viscosity and thermal diffusivity of the fluid.

The initial condition corresponds to the isothermal flow obtained at  $Re=110000$  and described in Serre *et al.* (2002).

## NUMERICAL METHOD

The numerical solution is based on a pseudo-spectral collocation, Chebyshev in both radial and axial directions ( $r, z$ ) and, in view of the  $2\pi$ -periodicity of the solution in this configuration, a Fourier-Galerkin method is used in the tangential direction. This choice takes into account the orthogonality properties of Chebyshev polynomials and, in particular, provides exponential convergence - referred to as spectral accuracy (Peyret 2002). The high-order accuracy of these methods ensures an accurate description of the secondary flows of weak intensity compared to the primary flow. Moreover, the use of the Gauss-Lobatto collocation corresponding to the extrema of the Chebyshev polynomials of high degree,  $N$  and  $M$  in the radial and axial directions respectively, directly ensures high accuracy of the solution within the very thin wall layers.

The differential equations are exactly satisfied at the Gauss-Lobatto collocation points,  $(r_i, z_j) \in [-1, 1] \times [-1, 1]$ :  $r_i = \cos(i/N), z_j = \cos(j/M)$  for  $(i=0, \dots, N$  and  $j=0, \dots, M)$ .

The solution  $(u, v, w, p)$  is approximated by a development in a truncated series:

$$\Psi_{NKM}(r, \theta, z, t) = \sum_{k=-K/2}^{k=K/2} \sum_{n=0}^N \sum_{m=0}^M \tilde{\Psi}_{nkm}(t) T_n(r) T_m(z) e^{ik\theta},$$

where  $T_n$  and  $T_m$  are the Chebyshev polynomials of degrees  $n$  and  $m, -1=r, z=1$  and  $0=\theta=2\pi$ . The physical conditions are explicitly taken into account at the boundaries.

The problem of velocity-pressure coupling has been overcome by the use of an improved projection scheme for time discretization. The improvement lies in the computation of the pressure predictor at each time step, which allows a possible variation of the normal pressure gradient at the

boundaries during the time integration. This version has been shown to reduce the slip velocity at the boundary and to produce second-order accuracy in time for the pressure. The time scheme is semi-implicit, second-order accurate. It corresponds to a combination of the second-order Euler backward differentiation formula and the Adams-Bashforth scheme for the non-linear terms.

All the DNS results presented in this work are performed at a rotational Reynolds number  $Re=1.1 \times 10^5$  ( $Re = \Omega R_1^2 / \nu$ ). The number of grid points used in this paper is  $128 \times 128 \times 128$ , in the radial, axial and tangential directions, respectively. The time step adopted is  $\delta t = 10^{-4}$  ( $10^4$  iterations per  $2\pi$  rotation). The solutions are grid independent for mean flow statistical quantities. A relevant measure of the solution accuracy, in the case of an incompressible flow, is to check that the flow is divergence-free. In the present computations, the divergence field is equal to  $4.10^{-10}$  within the domain and of the order of  $10^{-7}$  at the boundaries. Additional results regarding the convergence behaviour and the accuracy of the numerical method are given by Serre and Pulicani (2001).

The performance of the solver has been optimised with respect to vector-parallel supercomputer, here a Nec SX5 using 40 processors each with a memory of 224 Gbytes. The performance of the code is very high, about 6Gbytes, using 75% of the maximum ability of the computer. Such performance allows us to carry out time-dependent 3D computations with high resolution.

## NUMERICAL RESULTS

*Instantaneous data.* As in the case of an infinite disc (Serre *et al.* 2001), when the upper disc is impulsively started, a thin Ekman boundary layer is formed which acts as a pump drawing in fluid axially and driving it away in centrifugal spirals (this is sometimes known as ‘Ekman pumping’). In a closed container, this fluid swirls along the stationary vertical outer wall to the stationary disc. Then, the fluid spirals inward in the Bödewadt layer before again turning axially towards the rotating disc. Consequently, the base flow is of Batchelor type with both Ekman and Bödewadt layers separated by a non-viscous core rotating at constant angular velocity.

In this work the rotation is kept constant at  $Re=110\,000$  while the Prandtl number is chosen for air,  $Pr=0.7$ . In the principal cases to be presented the Rayleigh number is precisely zero ( $Ra = 0$ ). In Figure 1 we show a typical instantaneous field of velocity vectors and resultant isotherms along a meridional plane ( $r, z, \pi/4$ ). The instantaneous flow shows clearly a radially outward flow that, in this view, appears virtually laminar adjacent to the upper rotating disc. A more chaotic structure is created, however, after the flow has impinged on the outer shroud. The inward flow along the stationary disc is clearly turbulent. An interesting and abiding feature of this Bödewadt layer is that a particularly intense eddy is nearly always present about 50% of the distance from the shroud to the hub. The flow remains turbulent as it rises on the hub but after impact on the rotor surface the flow is rapidly smoothed out to the nearly laminar flow noted at the start of the cycle. Thus, as previously observed, there is a large difference between the Ekman and Bödewadt layers, laminar and turbulent flows coexisting within the cavity. The fact that the rotating boundary layer is close to laminar, is expected from the experiments of Itoh *et al.* (1992) where the rotating layer became turbulent only for  $Re_r = 3.6 \times 10^5$ .

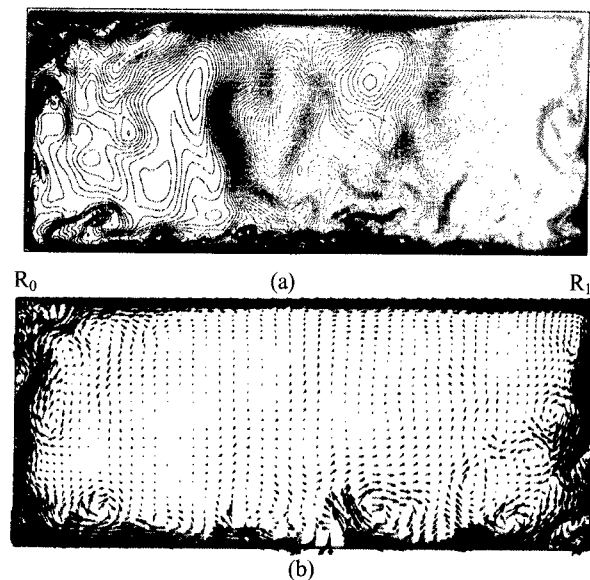


Figure 1: Instantaneous iso-lines of temperature (a) and velocity vector field (b) in the meridional plane ( $r, z, \pi/4$ ).

The flow pattern in the central core where the flow rotates in largely solid-body rotation is characterized by less intense but larger scale motions. Their impact can be seen most clearly from the chaotic isotherm pattern in Figure 1a. A striking impression of the change of scales is provided in Figure 2 which shows, in an isometric view of half the cavity (covering  $0 < \theta < \pi$ ), the imprint of the isotherm  $T = 0.65$  ( $T$  being unity at the lower wall and minus one on the rotor). Besides the upflow on the inner core one notices a large excursion of hot fluid towards the spinning upper disc transported by the large scale motions.

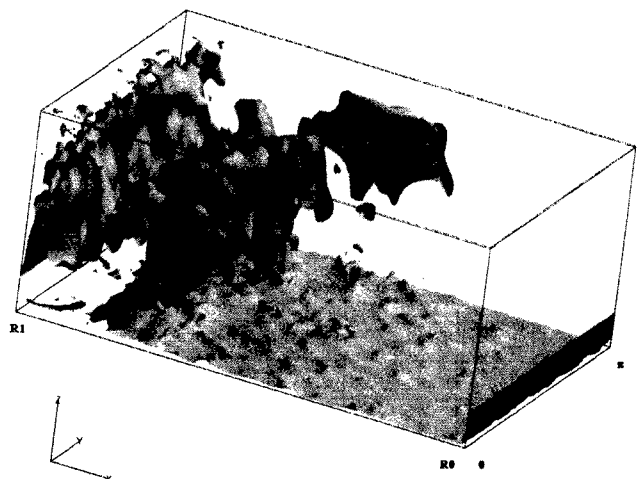


Figure 2: Instantaneous iso-surface of hot temperature  $T=0.65$  showed in a cartesian frame of reference.

Figure 3 focuses on the flow structure in the immediate vicinity of the two discs. For the rotor, at small radii one sees the imprint of the turbulent flow leaving the rotating hub. At about one fifth of the way across the annulus, however, there is a quite different structural changeover to persistent spiral structures which are very like the pre-transition vortices reported by Serre *et al.*, 2001 at lower Reynolds number and associated with the classic Ekman layer instability. A quite different pattern is evident near the stationary disc where the

imprints of the velocity vector normal to the disc indicate finer scale structures than on the rotor.

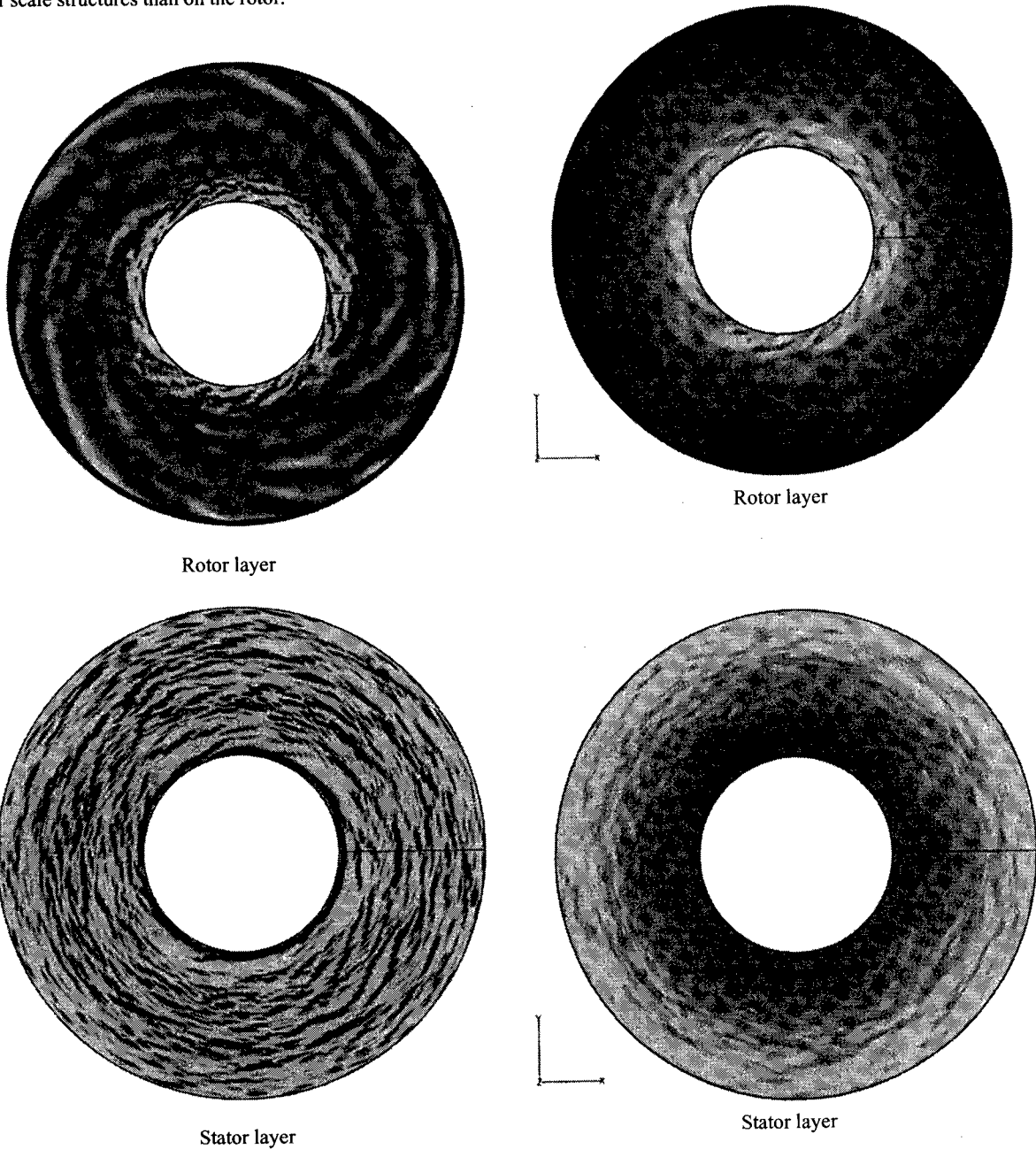


Figure 3: Instantaneous iso-lines of the axial component of the velocity in both rotor and stator layers showing the scale differences between the turbulent stationary disk layer and the laminar rotating disk layer.  $Re=110\ 000$ .

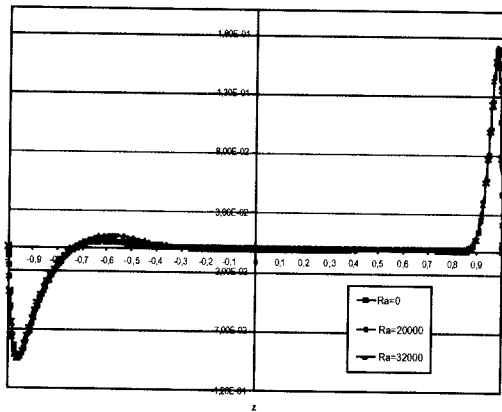
Moreover the structures are now more in the form of concentric circles than spirals. Figure 4 shows the corresponding instantaneous normal temperature gradient at the disc surfaces which is, of course, proportional to the local heat transfer rate through the surface. Although the grey scales do not correspond perfectly, it is clear that these heat-flux pictures reveal the same structure as seen in the views of instantaneous velocity direction. In other words (and unsurprisingly) the pattern of heat transfer rate is strongly affected by any organized structure in the flow pattern.

Figure 4: Instantaneous normal temperature gradient at the discs surfaces,  $Re=110\ 000$

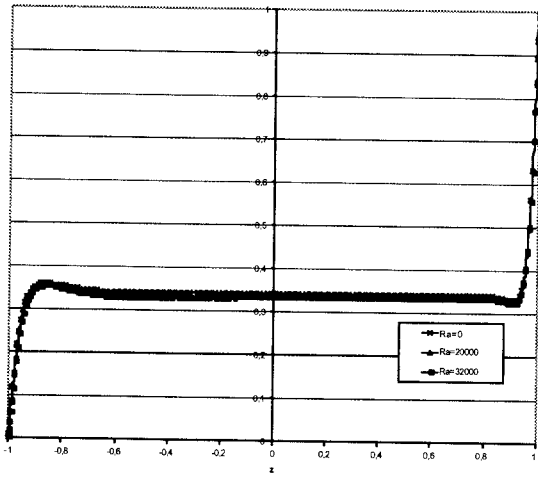
*Statistical data.* The statistical data presented in this section are averaged both in time and in the homogeneous tangential direction. The statistical steady state is supposed to be reached when the time fluctuations of the averaged values are less than 1%. In the present computations,  $5 \cdot 10^5$  time steps were required, that is a CPU-time of about 700 hours on the Nec-SX5. The averaged quantities are written using capital letters.

The distribution of the tangential and radial mean velocities across the gap between the discs is shown in Figure 5 at mid-radius. As found in experimental studies and broadly inferred by the instantaneous view (Figure 1b) the two discs boundary layers are separated by a core in solid body rotation. The difference in the thickness and shape of the radial velocity

profile near the two discs suggests that the stator layer is turbulent at mid-radius while the rotor layer remains laminar. That is the primary reason that the core circumferential velocity is only about one third of that of the rotor at the same radius. The corresponding mean temperature profile in Figure 6 exhibits the same form with an appreciably larger temperature drop across the nearly laminar rotor layer than across the turbulent stator layer.



(a)



(b)

Figure 5: Axial profiles of the mean velocity components at mid-radius and for three values of Rayleigh number. (a) Radial mean velocity,  $U$ . (b) Tangential mean velocity,  $V$ . The profiles are normalised with local angular velocity of the rotating disc  $\Omega \bar{r}$ .

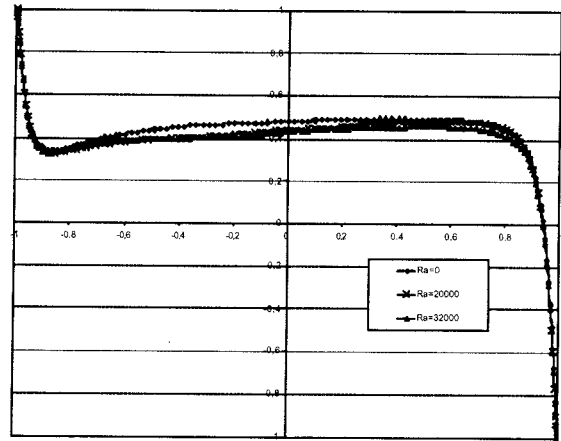
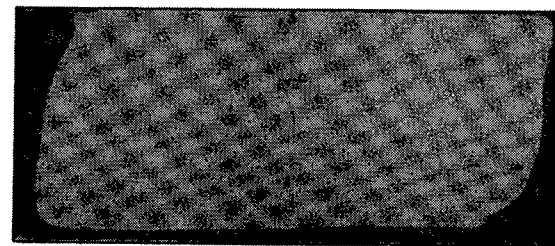
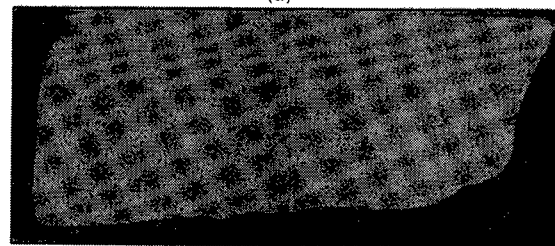


Figure 6: Axial profiles of the mean temperature at mid-radius and for three values of Rayleigh number.

*Inclusion of Force-Field Effects* As a preliminary to carrying out a detailed investigation of the effects of a force field on this swirling disc flow we have obtained results for a very mild density variation giving rise to a Rayleigh number based on the maximum radial acceleration ( $Ra = O^2 R_1 a^2 TH^3 / \rho$ ) up to 16,000. We have simultaneously included a gravitational field acting vertically down in the  $z$  direction such that the Froude number,  $Fr = O^2 R_1 / g = 0.5$ . The effect of adding these additional terms is just visible in the radial velocity profile shown in Figure 5 while the mean temperature in the core is marginally reduced, Figure 6. A somewhat more significant change is evident in the meridional map of turbulent kinetic energy shown in Figure 7. The inclusion of these force-field effects raises the turbulence energy appreciably in the down-flow on the shroud and along stator boundary layer. The effect on this latter surface seems likely to be due to the 'true' gravitational effect, that is, a heated horizontal surface warming and augmenting the fluctuations in the fluid passing over it.



(a)



(b)

Figure 7: Iso-lines of turbulent kinetic energy  $k$  in the meridional plane ( $r, z, \pi/4$ ). (a)  $Ra=0$ , (b)  $Ra=16,000$ .

## Acknowledgements:

The authors acknowledge the IDRIS/CNRS (Orsay) centre where the computations were carried out on Nec SX5 supercomputer. BEL's participation in this research has been possible with the support of the Royal Society's International Exchanges Scheme"

## REFERENCES

- Brady, J. F. and Durlofsky, L., 1986 "On rotating disc flow." *J. Fluid Mech.*, 175, pp. 363-394.
- Czarny, O., Iacovides, H. and Launder, B. E., 2003, "Precessing vortex structures in turbulent flow within rotor-stator disc cavities" *Flow, Turbulence & Combustion* (to appear)
- Elkins, C. and Eaton, J.K., 2000 "Turbulent heat and momentum transport on a rotating disk" *J. Fluid Mech.*, 402, pp. 225-253.
- Iacovides, H., and Toumpanakis, P., 1993, "Turbulence modelling of flow in axisymmetric rotor-stator systems," *Vth Int. Symp. On Refined Flow Modelling and Turbulence Measurements*, Paris, France, Sept. 7-10.
- Itoh, M., Yamada, Y., Imao, S., and Gonda, M., 1992, "Experiments on turbulent flow due to an enclosed rotating disc," *Expl Thermal Fluid Sci.* 5, pp.359-368.
- Owen, J. M., and Rogers, R. H., 1989, Heat transfer in Rotating Disc Systems, Vol. 1 : Rotor-stator Systems (ed. *W. D. Morris*), Wiley.
- Owen, J. M., and Rogers, R. H., 1989 "Heat transfer in Rotating Disc Systems", Vol. 2 : Rotating Cavities (ed. *W. D. Morris*), Wiley.
- Owen, J. M., 2000,"Flow and heat transfer in rotating disc systems CHT01," *Turbulence Heat and Mass Transfer* (ed. *Y. Nagano, K. Hanjalic and T. Tsuji*), Aichi Shuppan Press, pp. 33-58.
- Peyret, R. 2002 "Spectral methods for incompressible viscous flow", *Appl. math. sciences* 148, New-York Springer-Verlag
- Serre, E., Crespo del Arco, E., and Bontoux P., 2001 "Annular and spiral patterns in flows between rotating and stationary discs", *J. Fluid. Mech.* 434, pp. 65-100.
- Serre, E., and Pulicani, J. P., 2001 "3D pseudo-spectral method for convection in rotating cylinder," *Intl. J. of Computers and Fluids* 30/4, pp.491-519.
- Serre, E., Czarny, O., Iacovides, H., Bontoux, P. and Launder, B., 2002 "Precessing vortex structures within rotor-stator disk: DNS and visualization studies", *Advances in Turbulence IX*, pp. 421-424, CIMNE, Barcelona.
- Verzicco, R. and Camussi, R., 1999 "Prandtl number effects in convective turbulence" *J. Fluid. Mech.* 383, pp. 55-73.
- Yan, W.M. and Lee, K.T. 1997 "Unsteady conjugated mixed convection flow and heat transfer between two co-rotating discs", *Int. J. Heat Mass Transfer* 40 (12), pp. 2975-2988.